Mass Transport by Second Mode Internal Solitary Waves

Alan Brandt, PI
Johns Hopkins Univ. Applied Physics Laboratory
Laurel, MD 20723
phone: (240) 228-5915 fax: (240) 225-6908 email: alan.brandt@jhuapl.edu

Omar M. Knio, co-PI
Dept. of Mechanical Engineering & Material Science, Duke University
Durham, NC 27708
phone: (919) 660-5344 fax: (919) 660-8963 email: omar.knio@duke.edu

Award Number: N00014-12-01-0385
http://jhuapl.edu

LONG-TERM GOALS

The overall scientific objective of the proposed effort is to improve our understanding of the propagation and mass transport of internal solitary waves (ISW), particularly mode-2 ISW, and their significance for coastal ocean processes. In recent years numerous observations of mode-2 ISW have been reported so that it appears that such waveforms may be more prevalent than previously thought. Large amplitude mode-2 solitary waves have unique properties: in particular they encompass regions of internal recirculation that enable mass transport over large distances. Transport of mass along a pycnocline can affect upper ocean mixing and distribution of biological and chemical constituents. Moreover, coherent ISW packets can have significant effects on the propagation and scattering of acoustic signals.

OBJECTIVES

The objectives of the current effort are to: (1) improve our fundamental understanding of mode-2 ISW mass transport including the effects of ambient shear; (2) characterize the three-dimensional mass transport from localized sources; and, (3) use the results to aid in the interpretation of ocean observations and ascertain the implications for ocean mixing and bio-chemical transport.

APPROACH

Increased understanding of mass transport will be achieved by a combined series of numerical simulations and scaled laboratory experiments focused on determining the extent and persistence of ISW mass transport.

The numerical simulations of mode-2 ISW (O.M. Knio, Duke Univ.) are based on the Boussinesq model developed by Terez & Knio (1998) and recently extended by Salloum et al. (2012). The model integrates the mass and momentum conservation equations and simulates the motion of Lagrangian particles, used to characterize and quantify mass transport. Also modeled is the evolution of a passive

scalar and of a Lagrangian particle field, both used to analyze mixing and to compare predictions to experimental measurements. The extended model:

1. Accounts for the presence of current shear,
2. Accounts for the 3D evolution of a mode-2 ISW,
3. Incorporates higher-order discretization that would enable efficient computations of ISW at higher Reynolds numbers in order to more accurately simulate ocean conditions.

The laboratory experiments (A. Brandt, JHU/APL) extend earlier (Brandt, 2007) and more recent studies on ISW mass transport (Brandt et al., 2011) in the existing two-layer interfacial tank. Basic wavefield properties (amplitude, wavelength, etc.) are measured by imaging the evolution of the dye initially placed in the mixed generation region (Figure 1). Mass transport is determined by imaging the area of the dye included in the ISW bulge. Laser sheet imaging of fluorescent dye will be employed to ascertain the dynamics of the internal recirculation patterns in the large-amplitude ISW. PIV is also being employed to determine local velocities in the vicinity and within the ISW bulges. These studies:

1. Investigate the efficiency of various mechanisms for ISW generation and mass transport to simulate the candidate ocean forcing conditions.
2. Measure the effects of ambient shear flow on ISW generation/propagation process in the JHU/APL interfacial shear tunnel.
3. Investigate ISW mass transport and spreading in 3D, simulating the evolution of ISW in the coastal ocean in a 3D (square) stratified tank, to provide an understanding of the extent of mass transport and a comparison to the 2D case.

WORK COMPLETED

A manuscript on our experimental work on mode-2 ISW mass transport was published (Brandt & Shipley, 2014). Partial results of the results were presented at the APS DFD meeting (Shipley & Brandt, 2013). The work was also presented as invited papers (Brandt & Shipley, 2013; Brandt, 2014). In addition two manuscripts on the numerical simulations are in preparation (Rizzi et al, 2014; Li, et al, 2014a), and the most recent numerical results will be presented at the upcoming DFD APS meeting (Li et al, 2014b).

All experiments were conducted in the stratified shear tank of Figure 1 in which a thin interface was created between a lower layer of salt water (of various densities) and an upper layer of fresh water. Data from the series of laboratory experiments using different mechanisms for ISW generation and mass transport (to simulate the candidate ocean forcing conditions) conducted in FY13 were analyzed. The generation mechanisms investigated include:

- Mixed region release and collapse (“dam break”) – simulating front/intrusion ISW generation
- Oscillating mixer – simulating internal wave generated mixing
- Rotating paddle mixer – simulating internal wave instabilities
- Forced wedge displacement – simulating flow over a seamount.

Experiments were conducted to measure the recirculation patterns within the mode-2 ISW bulge using particle imaging velocimetry (PIV). These experiments are continuing.

On the computational side, our efforts have focused on:

- Development and validation of a direct numerical simulation (DNS) model was for the incompressible 3D Navier-Stokes equations in the Boussinesq limit utilizing high-order spatial and temporal discretizations.
- Utilization of this model to simulate 3D propagation of ISWs focusing on the effects of 3D instabilities and shear.

RESULTS

Representative images of the leading mode-2 ISW for different amplitude conditions are shown in Figure 2. While all the ISW generated were large-amplitude, i.e. had internal recirculating regions and transported mass, they generally were of three types depending on their amplitudes, a_b/h (a_b is the half-amplitude of the ISW and h is the characteristic pycnocline thickness), as shown in Figure 2. These can be classified as: $a_b/h < 2$, small-amplitude ISW with a smooth front face (Figure 2a); $2 < a_b/h < 4$, large-amplitude ISW with an open mouth, "PacMan" opening where external fluid was entrained into the bulge (Figure 2b); and, $a_b/h > 4$, very large-amplitude ISW again with smooth front face likely due to strong internal recirculation (Figure 2c). In the very large-amplitude waves, such as Figure 2c, local mixing instabilities are apparent at the ISW bulge aft end. Previous work on this grant included the first quantitative measurements of the mass transport by such mode-2 internal solitary waves propagating on a thin pycnocline (Brandt & Shipley, 2014).

Analysis of the laboratory experiments using different mechanisms for ISW generation and mass transport (to simulate the candidate ocean forcing conditions) showed that once the ISW was generated, its characteristics were indistinguishable between different generation mechanisms when the same amplitude wave was created (Figure 3). However, as can be seen in Figure 3, different generation mechanisms were found to produce significantly different wave amplitudes indicating different generation mechanisms result in different amounts of mass transport. For example, the paddle generation (simulating generation be internal wave instabilities) while the wedge (seamount generation) generates medium amplitude waves and the oscillator/box (intrusion generation) creates a wide range of amplitudes.

Figure 4 presents the velocity and vorticity fields measured with PIV at one location for a mode-2 ISW. The strong recirculation region can be seen including significant vorticity along the top and bottom edges of the bulge. Of note is the top to bottom asymmetry in the velocity/vorticity fields despite the fact that the dye visualization is relatively top/bottom symmetric suggesting a potentially complicated mechanism for mass entrainment and detrainment. Also of note is the weaker counter-rotating flow at the lower aft end of the bulge as well as weaker recirculation (indicating mode-2) in a trailing wave. The strong vorticity at the top aft end of the first bulge likely contributes to the roll-up instabilities in this region seen in slightly larger ISWs (e.g., Figure 2c) and the top/bottom asymmetry in which there is a lack of such vorticity at the lower aft end of the bulge could explain why this instabilities are seen primarily on the upper aft of the bulge and not the lower.

Work ongoing and planned for the balance of the current grant is focused on continuation of these PIV measurements of the velocity field of the recirculation within the bulge with and without an external shear flow.

A direct numerical simulation (DNS) model was developed for the incompressible three-dimensional Navier-Stokes equations in the Boussinesq limit. The numerical scheme relies on a pressure-projection method with high-order discretizations in both space and time. In addition, a high-order WENO scheme is adopted for convection terms to preserve mass conservation properties. The numerical code was first validated by simulating both 2D lock-exchange and 3D Holmboe instability problems. The validated code was applied to simulate 3D propagation of ISWs originating from the collapse of a centered mixed mass. The simulations were designed to address the impacts of 3D instabilities as well as background shear, on ISW-induced mass transport and mixing processes.

Results indicate that, compared to 2D simulations, the flow energy dissipates more rapidly in three dimensions, and the growth of 3D instabilities (Figure 5) slightly inhibits mass transport and mixing rate. The results also indicate that the leading wave bulge is mostly maintained by the entrainment of mixed mass along the pycnocline. Associating a "roughness" measure of density fields (where "roughness" is defined as the standard deviation of density field along the spanwise direction) with mass mixing enables identification of the area where most of the spanwise mixing process takes place, and the spatial extent of this mixing area. Simulations show that the spanwise mixing process evolves almost linearly with time and that around 50-60% of the initial mixed region is involved in the spanwise mixing. In addition, similar to observations in previous 2D simulations (Rizzi et al, 2014), it is found that strong background shear (smaller shear thickness) leads to more efficient mass transport and mixing

IMPACT/APPLICATIONS

Transport of mass along a pycnocline can affect upper ocean mixing and distribution of biological and chemical constituents. Coherent ISW packets can also have significant effects on the propagation and scattering of acoustic signals. The present fundamental investigation of mode-2 ISW can aid in interpretation of ocean observations of ISW and their mass transport effects.

TRANSITIONS

The results of this effort will be transitioned to Navy programs concerned with ocean wave dynamics and vehicle signatures.

RELATED PROJECTS

ONR Code 331 study of Body Generated Internal Waves. This study complements the present effort by relating basic oceanographic processes to those involving wave generation by Navy assets.

REFERENCES

Brandt, A. 2007 "Evolution of Mode-2 Solitary Internal Waves in a Stratified Shear Flow." Fifth Int. Symp. on Environmental Hydraulics (ISEH V), Tempe, AZ, 4-7 December 2007, 6 pp.

Brandt, A. 2014 "Mass Transport by Large and Very-large Amplitude Mode-2 Internal Solitary Waves: Experimental Observations." Invited seminar, Nonlinear Dynamics Seminar, Univ. Texas, Austin, 13 October 2014.

Brandt, A. & Shipley, K.R, Salloum, M. & Knio, O.M. 2011 "Mass Transport by Large Amplitude Internal Solitary Waves," 64th Annual Meeting of the Am. Phys. Society Division of Fluid Dynamics (DFD), 20-22 November 2011, Baltimore, MD.

Li, G., Rizzi, F., O. M. Knio, 2014a "Three-dimensional simulations internal solitary waves," in preparation.

Li, G., F. Rizzi, O. M. Knio, 2014b "Three Dimensional Simulations of Internal Solitary Waves," accepted for presentation, 67th Annual APS DFD Mtg, San Francisco, CA, November 23–25, 2014.

Rizzi, F., G. Li, O.M. Knio, A. Brandt, 2014 "Numerical Simulations of Deep Density Currents," in preparation.

Salloum, M., Knio, O.M., Brandt, A., 2012 "Numerical Simulation of Mass Transport in Internal Solitary Waves," *Phys. Fluids,* 24, 016602; doi: 10.1063/1.3676771.

Terez, D.E., Knio, O.M., 1998 "Numerical simulations of large-amplitude internal solitary waves", *J. Fluid Mech. 362,* 53-82.

PUBLICATIONS

Brandt, A., Shipley, K. 2013 "Mass transport by large and very-large amplitude mode-2 internal solitary waves: experimental observations," invited presentation, 3rd DNVA-RSE Norway-Scotland Waves Symposium, 16-17 September, Oslo, Norway. [published (extended abstract), invited]

Brandt, A., Shipley, K. 2014 "Laboratory Experiments on Mass Transport by Large Amplitude Mode-2 Internal Solitary Waves," *Phys. Fluid. 26*(4), 046601. [published, refereed]

Li, G., F. Rizzi, O. M. Knio, 2014b "Three Dimensional Simulations of Internal Solitary Waves," accepted for presentation, 67th Annual APS DFD Mtg, San Francisco, CA, November 23–25, 2014.

Shipley, K., Brandt, A. 2013 "Mass transport by large & very-large amplitude mode-2 internal solitary waves: experimental observations," 66th Annual Mtg, Am. Phys. Society Div. of Fluid Dynamics (DFD), 24-26 November 2013, Pittsburgh, PA.

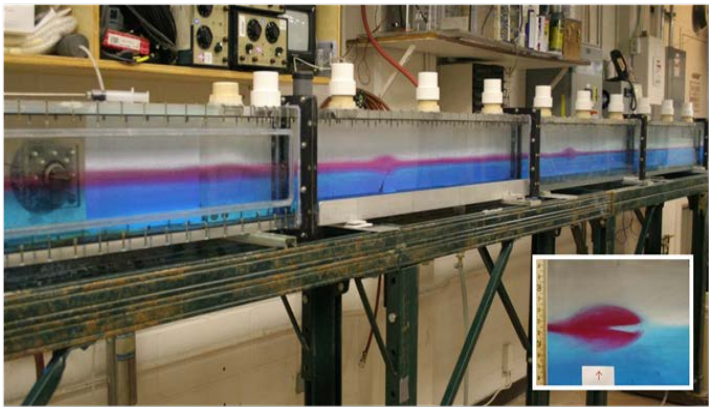

Figure 1. Stratified shear tunnel showing mode-2 ISW propagating on the thin interface (red). Upper clear layer is fresh water; bottom, blue layer is high density salt. Inset shows enlargement of a large amplitude ISW entraining fluid at the leading edge resulting in the characteristic "Pac-Man" pattern.

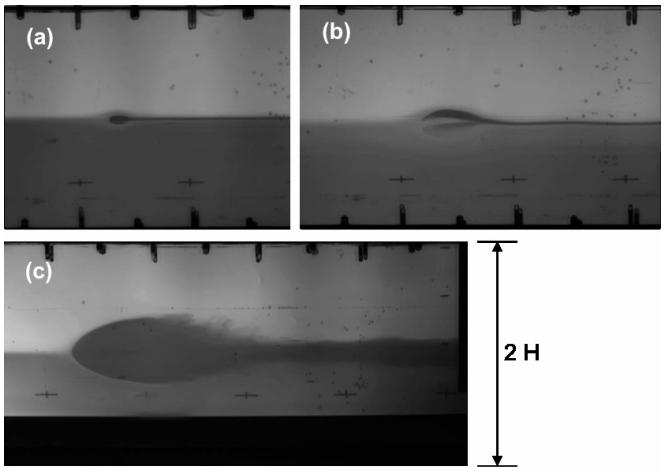

Figure 2. Black and white images of representative ISW bulges: (a) lower amplitude, a_b/h = 0:68; (b) large amplitude, a_b/h = 1:96; (c) very-large amplitude, a_b/h = 5:92. Here, a_b is the bulge half amplitude and h is the characteristic half-thickness of the interface layer. (Taken from Brandt & Shipley, 2014.)

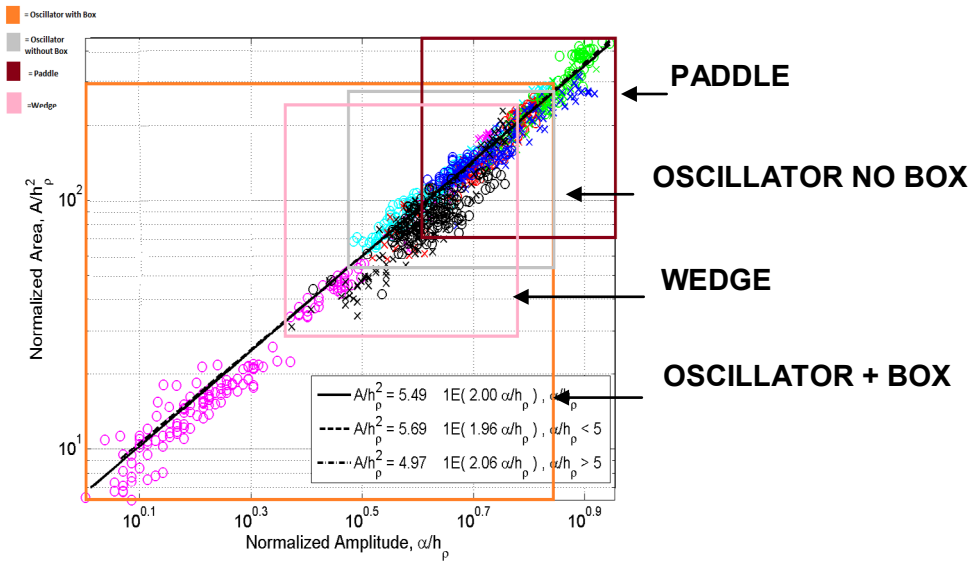

Figure 3. Plot of normalized ISW area (a proxy for mass being transported) vs. normalized amplitude for four different generation mechanisms. As can be seen, all the data collapse onto the same relation independent of generation mechanism. However, each mechanism more readily generates different sized waves and thus results in different amounts of mass transport.

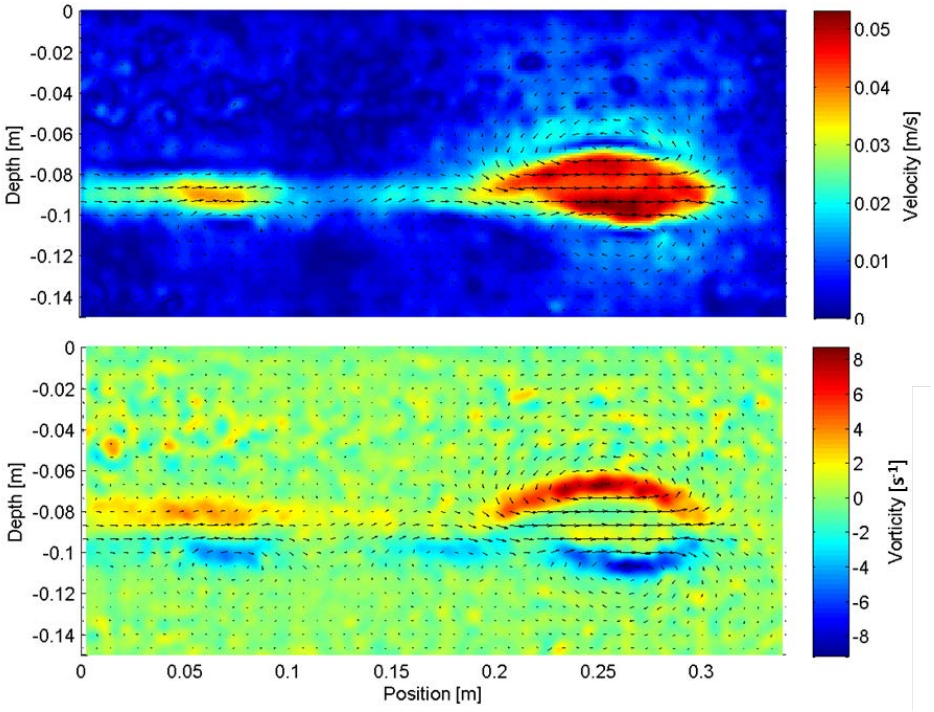

Figure 4. Instantaneous velocity and vorticity flow fields measured with PIV for leading and first following mode-2 ISW propagating from left to right ($a_t/h = 3.2$). Shown are contours of velocity magnitude (top) and span-wise vorticity (bottom) overlaid with velocity vectors (both top and bottom).

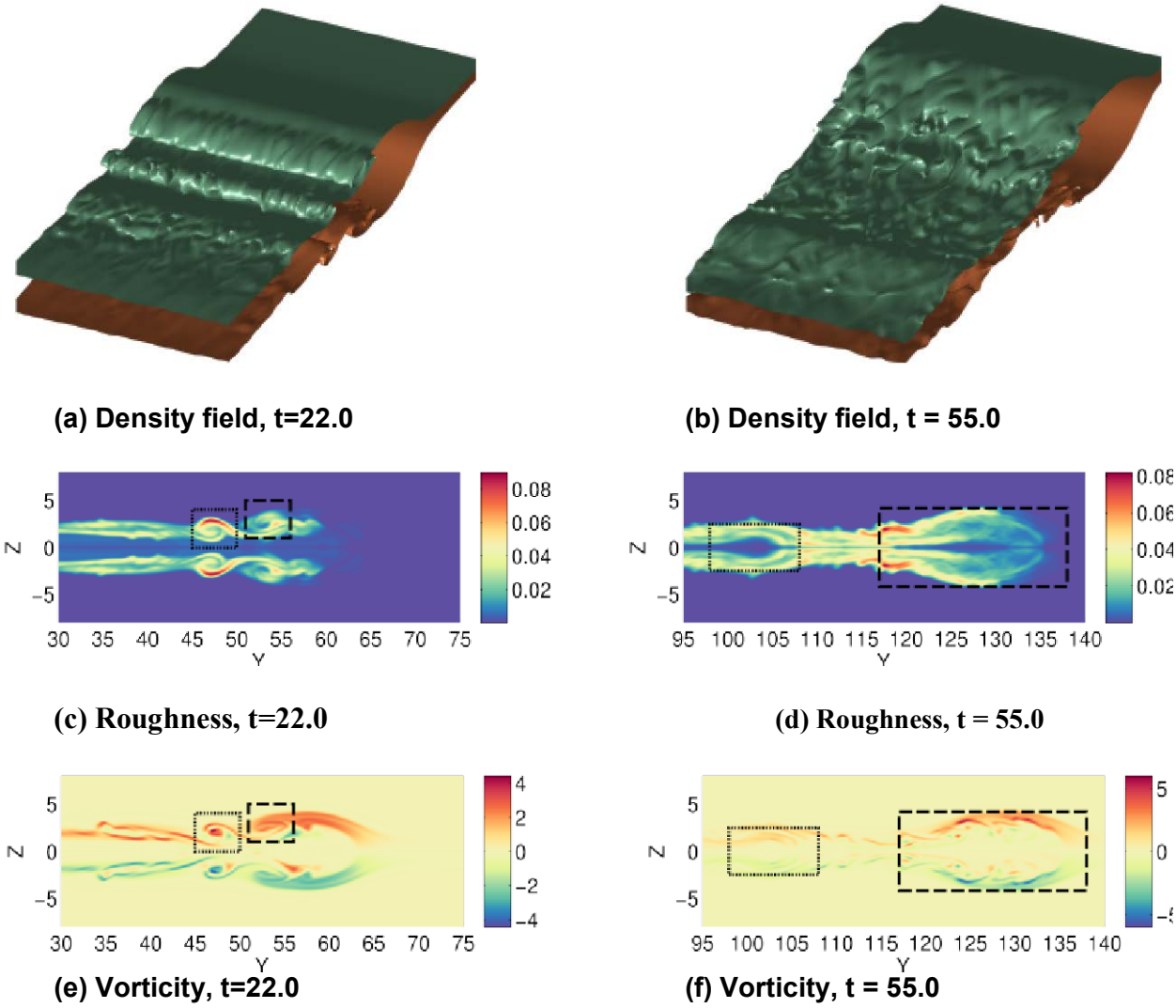

Figure 5. Instantaneous snapshots of the 3D density field, roughness and vorticity in spanwise plane at selected times computed with new 3D DNS code.